Transfer Learning-driven Biofield Image Analysis for Predictive Modeling of Diabetes

Shivanand S. Gornale, Supriya Shankar Patil, Anup Waman Deo[1], Abdulgaphur Athani[2]

Department of Computer Science, School of Mathematics and Computing Sciences, Rani Channamma University, Belagavi, Karnataka, [1]Institute of Biofield Evaluation and Research Centre, Thane, Maharashtra, India, [2]Department of Engineering Technology, University Technical Malaysia Melaka, Melaka, Malaysia

Abstract

Background: The human biofield serves as an indicator of an individual's physical and emotional health status. Biofield-based therapeutic techniques, also known as complementary and alternative medicine (CAM) techniques such as Reiki, Therapeutic Touch, and Pranic Healing, leverage this information in the preliminary assessment phase before treatment initiation. These modalities are increasingly integrated as complementary methods within health diagnostic frameworks. Among the techniques employed for biofield visualization, gas discharge visualization (GDV) and polycontrast interference photography (PIP) are the predominant imaging methodologies. Notably, the majority of scientific investigations and empirical studies have primarily utilized GDV-derived images, with comparatively fewer studies focusing on PIP-based data. **Purpose:** The primary objective of this study is to identify energy imbalances within the pancreatic region using biofield imaging and to utilize these patterns for classifying subjects as diabetic or nondiabetic. This work emphasizes the relevance of biofield information in health assessment and evaluates its potential for supporting energy-based diagnostic approaches. **Materials and Methods:** Color-based clustering methods were applied for segmentation. A transfer learning-based ensemble framework was developed using pretrained convolutional neural network (CNN) architectures ConvNeXtBase and ResNet50 to classify biofield images into diabetic and nondiabetic categories. Grid search optimization identified the optimal hyperparameters, which were applied during fine-tuning to improve feature learning. Ensemble model was evaluated, with the ConvNeXtBase + ResNet50 combination achieving the highest accuracy of 99.12%. Robust performance validation was ensured using 5-fold cross-validation to minimize sampling bias and enhance generalization. **Results:** The ensemble of ResNet50 and ConvNeXtBase achieved the highest accuracy of 99.12%, outperforming individual models (ConvNeXtBase: 97.93% and ResNet50: 96.28%). Receiver operating characteristic analysis confirmed strong reliability with area under the curve values above 0.99 for both classes (diabetic and nondiabetic). The 5-fold cross-validation analysis further demonstrated the robustness of the proposed ensemble model, achieving a mean accuracy of 97.45%, indicating highly consistent performance across different dataset partitions. **Conclusions:** The CNN-based models can be trained to classify the biofield images, and this approach can enable automated analysis of biofield images. The approach of using clustering, deep learning, and ensemble modeling as analyzed and described in this study seems to be highly effective. The overall system of biofield imaging and automated clustering can act as a potential noninvasive diagnostic support tool, though further testing with larger datasets and expert validation is necessary for clinical application.

Keywords: Biofield image, clustering image segmentation, deep learning techniques, gas discharge visualization, hyperparameter tuning, pancreas energy, polycontrast interference photography, transfer learning techniques

Received on: 14-09-2025 **Review completed on:** 12-12-2025 **Accepted on:** 13-12-2025 **Published on:** 31-03-2026

Introduction

Human biofield is formed around our body as a result of energy flow in the body. During this energy flow, photons are emitted, which helps in revealing the physical, emotional health of an individual. Recent advances in technology have enabled the noninvasive visualization of this biofield using specialized imaging techniques. One prominent method is polycontrast interference photography (PIP), an advanced digital scanning system that captures the energy field in the form of different colors, each corresponding to the frequency of photon emissions from various regions of the body.[1]

Access this article online

Quick Response Code:

Website: www.jmp.org.in

DOI: 10.4103/jmp.jmp_245_25

Address for correspondence: Ms. Supriya Shankar Patil, Department of Computer Science, School of Mathematics and Computing Sciences, Rani Channamma University, Belagavi, Karnataka, India.
E-mail: supriyapatil8409@gmail.com

How to cite this article: Gornale SS, Patil SS, Deo AW, Athani A. Transfer learning-driven biofield image analysis for predictive modeling of diabetes. J Med Phys 2026;51:136-44.

In this technique, a customized digital camera is used within a specially designed environment, as shown in Figure 1a, optimized for minimal electromagnetic interference and controlled lighting. Figure 1b shows the image captured and presented in the form of various colors. The interpretation of the biofield for health diagnosis is often based on the colors that appear on and around the body.[2-4] The colors on the body, known as the inner aura, and the colors surrounding the body, referred to as the outer aura, provide valuable insights. Many energy healing techniques utilize this information to identify the root cause of a disease.

These images are analyzed to assess both current health conditions and latent imbalances. Unlike conventional diagnostics, which typically detect disease only after at least 20% of physical manifestation, biofield scanning enables early intervention. By identifying energetic disturbances early, one can prevent the progression of disease, reducing both physical and financial burdens.

Biofield imaging techniques are commonly interpreted by trained energy practitioners who manually assess the chromatic and spatial patterns observed in the captured images. Each color within the image is thought to correspond to specific physiological or psychological states[1] based on established interpretive frameworks used in energy medicine. While effective, this approach is inherently subjective and lacks scalability due to its dependence on expert intuition.

Given the visually discernible and repeatable nature of color patterns in biofield images, computational methods offer an opportunity to automate the interpretation process.[5] Since color distribution plays a critical role in diagnosis,[2-4] unsupervised clustering-based segmentation methods are well-suited for isolating meaningful regions in the image. These methods allow for the extraction of dominant chromatic clusters that can serve as high-level features for downstream classification.

This integrated approach enables a reproducible, data-driven alternative to manual analysis by combining unsupervised segmentation with classification. The methodology leverages the strengths of both classical clustering algorithms for feature localization and state-of-the-art convolutional neural networks (CNNs) for high-accuracy image classification.

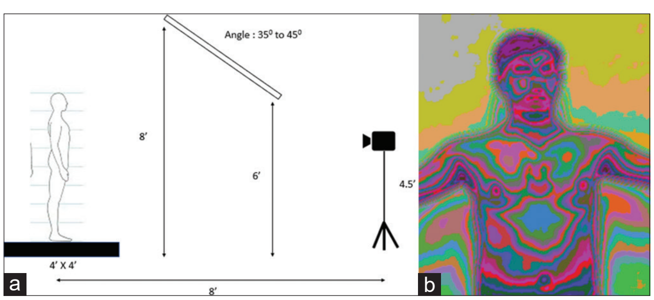

Figure 1: (a) Environment setup[1] representing alignment of camera, light source, and person to be scanned and (b) an example of biofield image captured using polycontrast interference photography

Detailed descriptions of the segmentation pipeline, model architectures, training protocols, and evaluation metrics are provided in the subsequent sections.

Key contributions of the study

1. Preparation of the dataset of biofield images – Pancreas Energy (PE24)
2. The most significant contribution of this study is the development of a soft-voting ensemble integrating ConvNeXtBase and ResNet50, which strategically combines two fundamentally different deep learning architectures for biofield image dataset PE24
3. Classifying images for the prediction of diabetes based on energy information at the pancreas region.

Related work

References to the biofield can be traced back to ancient literature, where it was reportedly used for healing. Modern methods such as Kirlian photography, resonance field imaging, and PIP now enable the capture of biofield information, which is utilized to analyze various health conditions. This section summarizes research emphasizing the significance of biofield information, the effectiveness of energy-based treatments, and various experiments conducted on biofield images.

Rubik *et al*.[6] reviewed the evolution of biofield science, highlighting its roots in ancient healing traditions and its growing relevance in modern complementary and alternative medicine (CAM). The biofield, viewed as an organizing principle for life and health, strengthens therapies such as acupuncture, energy healing, magnet therapy, and bioelectromagnetic treatments. The study emphasizes its significance in diagnosis, treatment, and as a theoretical framework for advancing research on mind–body interactions within biophysics and biology.

Bryndin and Bryndina[7] describe the biofield as closely connected to the body's physiological and energetic processes, generated by energy flows at key power centers. They note that health disturbances manifest as biofield imbalances, while restoration of these flows supports healing. Furthermore, variations in color patterns within the biofield are interpreted as indicators of behavioral traits, emotional states, and specific physiological or psychological conditions.

Joy *et al*.[8] enumerate a variety of energy healing techniques designed to harmonize the human biofield, including Reiki, Healing Touch, Pranic Healing, Qigong, Quantum Touch, Distance Healing Intention, Polarity Therapy, Johrei, Reconnective Healing, and Intuitive Healing. They advocate for future research integrating artificial intelligence (AI) tools to analyze biofield patterns. Such technologies could enhance early detection of energetic imbalances, potentially predicting health conditions earlier than conventional diagnostic methods.

Shanmugapriya and Rajesh[9] analyzed Kirlian fingertip images of 25 subjects, focusing on the inner and outer aura regions that correspond to organ health. Discontinuities in the inner aura and variations in the outer flame-like area were used as diagnostic indicators. To improve image clarity, morphological filtering was applied, followed by extraction of diagnostic features such as area, size, pixel count, connected components, and zero-crossing measures, which aided in health status interpretation.

Chiang Lee *et al*.[10] assessed bioenergy captured using gas discharge visualization (GDV) system of healthy individuals and stroke patients using parameters such as uniformity, mean dullness, average dullness, fractality dimensions, and fragments. Their findings showed clear differences between groups: healthy subjects exhibited continuous, high-intensity bioenergy flow with strong contrast, whereas stroke patients displayed disrupted and discontinuous energy fields in regions associated with the affected organs.

Srivastava *et al*.[11] in their study explore the effectiveness of chakra balancing in enhancing physical well-being. The authors observed that energy imbalances in various chakras are linked to physical and mental ailments such as diabetes, headaches, anxiety, and insomnia. The treatment plan focused on balancing the affected chakras through specific interventions, including chanting beej mantras, pranayama, guided meditation, mudras, and affirmations. Posttreatment comparisons of medical reports indicated significant improvements in the participants' physical well-being.

According to traditional Chinese medicine, cancer develops due to energy deficiencies and heat retention. Huang's[12] observations of cancer patients revealed a significant deficiency in chakra energy. Replenishing this energy has been found to aid in the improvement or potential cure of cancer.

Yakovleva *et al*.[13] conducted a pilot study involving 137 volunteers to analyze electrophotonic images (EPIs) for detecting colon tumors. The study utilized 69 parameters associated with the coccyx, sacrum, descending colon, and lumbar regions for classification. The results demonstrated sensitivity and specificity values of 76.4% and 85.0%, respectively.

Narayanan *et al*.[14] proposed unified system of medicine where EPI readings were recorded using Bio-Well device. Three parameters, namely energy of communication (C), total available energy referred as integral area (IA), and amount of coherence of energy referred as entropy, were used in their study. Subjects with abnormal values for these parameters were suggested to practice yoga. After the said duration in most of the cases, readings for the parameters C, E, and IA were found normal.

Chhabra *et al*.[2,3] developed the aura color space visualizer algorithm, which detects the human aura and provides insights into individuals' mentality, potential health issues, reactions to situations, and compatibility with others. The accuracy of their interpretations was validated through interviews with the subjects.

The research of Chhabra *et al*.[4] aimed to transform human emotions through sound healing therapy and validate the results by observing visible changes in human biofield. The study integrated image processing and machine learning techniques, incorporating real-time aura visualization and an emotion detection classifier to identify the emotions of participants. Experimental results demonstrated the effectiveness of the approach, achieving approximately 88% accuracy in the combined emotion and aura module.

An algorithm was proposed by Gornale *et al*.[5] to detect energy imbalances in the knee region from biofield images captured using an advanced digital scanning system that represents the human biofield through various colors. The method utilized contour and gray level co-occurrence matrix (GLCM) features, with support vector machine (SVM) and K-Nearest Neighbor (KNN) classifiers categorizing the images into three levels: high-, medium-, and low-energy imbalance. The classification achieved accuracies of 87.14% for SVM, 94.28% for KNN with $k = 3$, and 92.85% for $k = 5$.

The review of related work highlights that the human biofield provides insights into an individual's physical and mental health. Biofield-based therapy is being increasingly adopted as complementary tools into health diagnosis. Common therapies include Reiki, Therapeutic Touch, and Pranic Healing, which utilize information about energy blockages before initiating treatment. In various experiments, a significant number of patients reported noticeable improvements in stress levels, mental clarity, and physical ailments after undergoing biofield therapy.

It is also observed that many of the research studies have been conducted on images captured using GDV also referred as Kirlian photography, but PIP remains largely underexplored in computational science. To date, research using PIP has been limited to qualitative visual analysis, lacking systematic image processing, or machine learning frameworks. Moreover, public datasets or segmentation benchmarks are currently unavailable for PIP-based imaging, which presents a significant research gap. Hence, this study aims to address these issues.

Materials and Methods

The primary objective of the present study was to detect energy imbalances in the pancreatic region, which may assist in the early diagnosis of diabetes. As shown in Figure 2, the proposed methodology involved the use of clustering techniques for image segmentation, enabling the identification of distinct color-based clusters within biofield images. These segmented regions, particularly those corresponding to the pancreas, were subsequently utilized for classification using deep learning algorithms.

Dataset description

Images used in this experiment were collected from Institute of Biofield Evaluation and Research Centre (IBERC), Thane. The technique and setup for image acquisition were developed and patented by IBERC. Furthermore, a method for image analysis and identification of clinical finding based on various

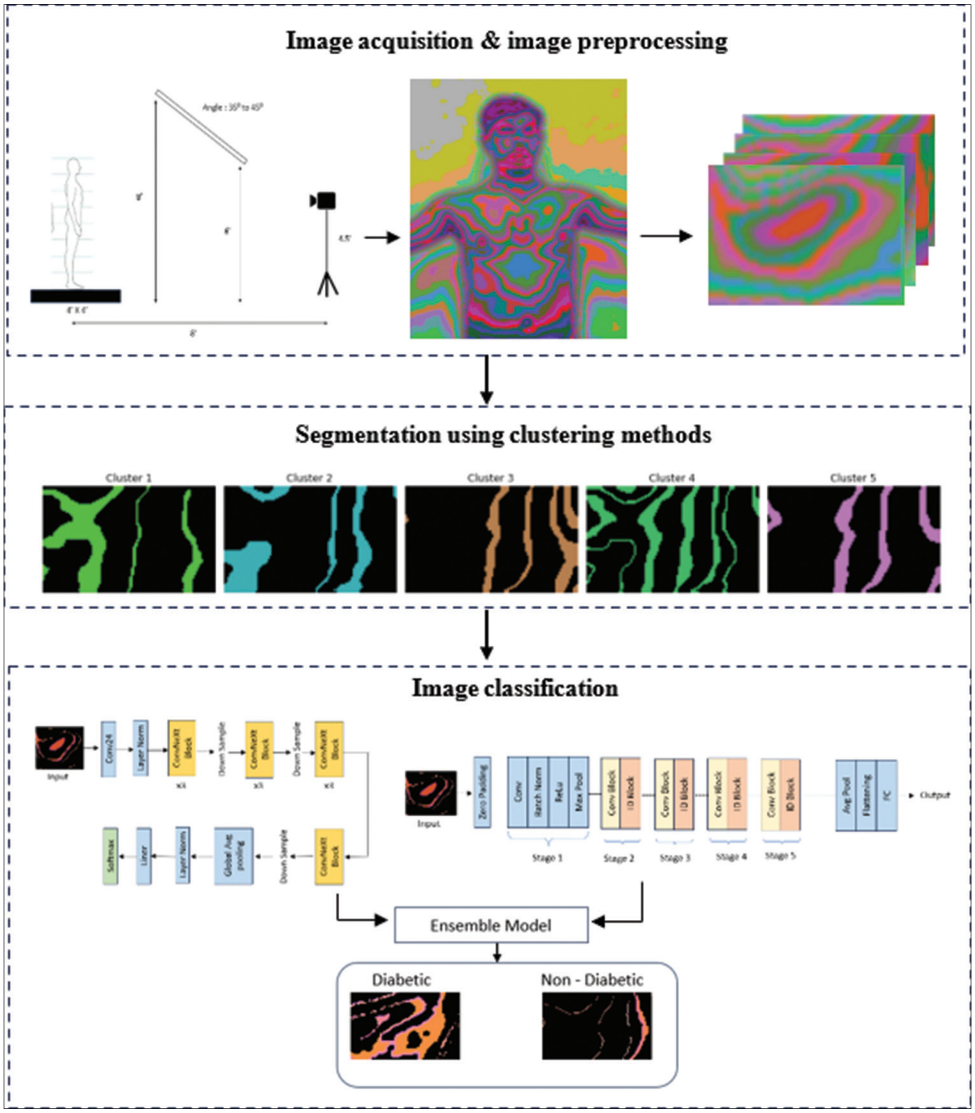

Figure 2: Block diagram of the proposed methodology illustrating the sequential workflow, including image acquisition and preprocessing, segmentation into multiple clusters, and the selection of relevant segmented regions for final classification into diabetic and nondiabetic categories

color schemes was developed by IBERC. This patent was filed on November 19, 2018, and after extensive data analysis, it was granted on March 15, 2024, with Patent No. 528035 by Indian Patent Office. Images were captured using the PIP technique, which captures the energy field around the human body and stores it as color images. The images captured were of resolution 1152 × 768 pixels and stored in Portable Network Graphics format. For a health diagnosis, the entire biofield around the subject was captured by taking around 35 photographs of each subject in different poses, capturing complete information. Publishing and sharing these images raises privacy concerns, as the imaging process typically involves capturing photographs of subjects in minimal clothing to ensure accurate visualization of energy emissions without interference from clothing or accessories. In this work, side profile images of 455 volunteers were used. The region required for early diagnosis of diabetes was extracted from the original images and was stored separately. Under the guidance of expert in biofield evaluation from IBERC, these were separated as 223 diabetic and 232 nondiabetic images.

Image segmentation using clustering

To isolate meaningful regions within the biofield image, unsupervised clustering techniques were employed for segmentation. The goal was to differentiate clusters based on color variations that potentially indicate energy concentrations or imbalances. The various clustering algorithms were analyzed for segmentation, such as K-means[15] clustering, mean shift, Gaussian mixture models,[16] simple linear iterative clustering,[17] DBSCAN,[18] and agglomerative clustering.[19] Based on the evaluation metrics computed, Silhouette score,[20,21] Calinski–Harabasz index,[22] and Davies–Bouldin index,[23] the mean shift clustering techniques exhibited the most promising results for segmenting biofield images. Following segmentation, only the target cluster representing the region of diagnostic importance, as shown in Figure 3, was extracted and retained for subsequent classification and analysis.

Image augmentation

Prior studies showed that augmentation significantly improves the performance of deep learning models, particularly in medical imaging contexts where data are often limited.[24,25] In this work, augmentation operations such as horizontal flipping, vertical flipping, rotation, shearing, and zooming were applied. After the augmentation, the dataset increased to 1115 and 1160 images of diabetic and nondiabetic classes, respectively. These techniques helped simulate real-world variations in image data and reduce the risk of overfitting by diversifying the input distribution without the need for additional data collection.

Model architectures

Transfer learning is a powerful deep learning strategy that enables a model trained on one task to be reused for a new, often domain-specific task. In image classification, transfer learning typically involves using CNNs that have been pretrained on large-scale natural image datasets such as ImageNet, which contains over 1.2 million images across 1000 classes. These pretrained models learn hierarchical filters in the early layers that capture fundamental visual patterns, including edges, shapes, textures, and spatial relationships features that remain useful even when the imaging modality or application changes.[26]

In contrast to training a model from scratch, which requires extensive labeled data and computational time, transfer learning offers several advantages, such as faster convergence, improved generalization, reduced overfitting, and enhanced performance, particularly when labeled data are limited.[27] This is especially beneficial in healthcare applications, where data collection is costly, expert annotation is resource-intensive, and patient privacy restricts dataset growth.[28]

ConvNeXtBase

Figure 4 illustrates the ConvNeXtBase architecture adapted for our biofield dataset. Inspired by hierarchical design strategies from modern vision transformers, ConvNeXtBase employs a purely convolutional backbone[29] with enhanced optimization and scalability characteristics. The stem layer utilizes a 4×4 convolution with a stride of four to downsample the input image and initiate hierarchical feature extraction. The model consists of four main stages with progressively increasing channel dimensions, each containing multiple ConvNeXt blocks that integrate depth-wise convolution, layer normalization, and point-wise convolution operations to efficiently capture both local texture and global structural information. A gaussian error linear unit (GELU) activation facilitates smoother nonlinear transformation at each block output. Like ResNet50, a global average pooling layer aggregates high-level feature maps into a low-dimensional vector, which is ultimately passed through

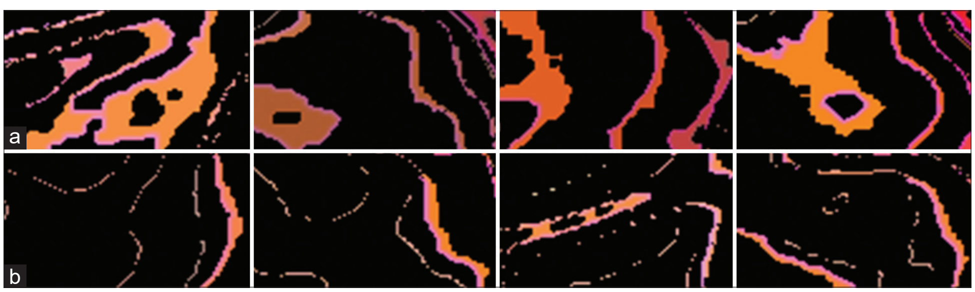

Figure 3: Extracted segmented images used for diagnostic interpretation. (a) Diabetic subjects exhibiting localized energy blockages represented by denser and thicker clustered regions. (b) Nondiabetic subjects showing relatively thinner regions showing less blockage

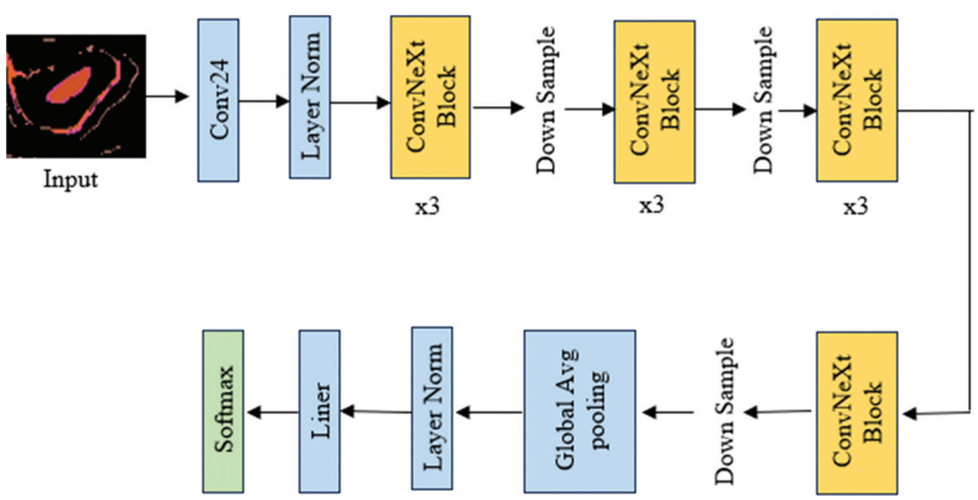

Figure 4: ConvNeXtBase backbone architecture integrated for feature extraction and classification, featuring repeated ConvNeXt blocks across four stages with increasing channels, followed by global average pooling and a softmax classifier

a fully connected classifier head to distinguish diabetic from nondiabetic patterns in the PE24 biofield dataset.

ResNet50

The architecture of ResNet50[30] is presented in Figure 5, where a deep residual learning framework is adopted to enable effective feature extraction while mitigating gradient vanishing in deeper networks. The model begins with a convolutional stem consisting of a 7 × 7 convolution with a stride of two, followed by a max-pooling layer to progressively reduce spatial dimensions while preserving key visual information. Four sequential residual stages are employed, each containing multiple bottleneck residual blocks composed of a 1 × 1 dimensionality-reduction convolution, a 3 × 3 spatial convolution, and a 1 × 1 dimensionality-expansion convolution. Skip connections directly feed feature maps from the input of each block to its output, ensuring improved information flow across layers. The final stage incorporates a global average pooling layer to compress the learned feature maps into a compact representation, followed by a fully connected layer with softmax activation to perform binary classification for diabetes prediction from pancreas-region biofield images.

Ensemble learning strategy

Ensemble modeling is a powerful machine learning approach that integrates multiple predictive models to improve overall performance, robustness, and generalization ability compared to individual models. It is increasingly recognized as a robust technique for boosting diagnostic performance in deep learning-based medical image analysis.[31,32] Typically, ensemble methods operate by combining outputs from different models using techniques such as majority voting, averaging, or stacking.[33] In this work, a stacking ensemble strategy[34] is implemented, where softmax outputs from two strong pretrained classifiers – ConvNeXtBase and ResNet50 – are ensembled for the prediction of diabetes.

Results

In this experiment, we evaluated a range of color-based clustering algorithms to segment the biofield images into meaningful and coherent regions. These algorithms operated by grouping pixels with similar color intensities, thereby enabling the separation of distinct energy zones or patterns within the pancreatic region. Among all the clustering techniques examined, mean shift clustering demonstrated the most reliable and consistent performance. Its ability to adapt to the underlying data distribution without requiring a predefined number of clusters allowed it to capture energy variations more accurately than other methods. As a result, mean shift emerged as the most effective approach for isolating relevant energy patterns in this study.

This study evaluated five individual transfer learning models and five soft-voting ensemble combinations for diabetic versus nondiabetic classification using biofield images. To identify the most effective learning configuration for each model, a systematic grid search strategy[35-37] was conducted on five CNN architectures: Xception, CNN, VGG16, ResNet50, and ConvNeXtBase. The search evaluated combinations of key hyperparameters including batch size (16, 32), learning rate (0.001, 0.0001), and optimizer (Adam, SGD), with all models trained for 20 epochs using binary cross-entropy loss. The hyperparameter set that achieved the highest validation accuracy was selected for subsequent fine-tuning and ensemble development. Overall, the grid search results consistently indicated that a learning rate of 0.0001, a batch size of 16, and the Adam optimizer provided the most stable convergence and improved classification performance. Performance details presented in Table 1 demonstrate that the initial results obtained using the original dataset were not satisfactory, highlighting the limitations in the model's capacity to generalize due to restricted data diversity. By

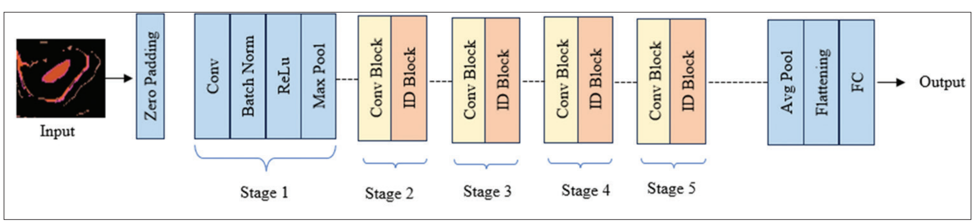

Figure 5: Detailed pipeline of the ResNet50 backbone, showing zero-padded convolutional stem, residual stages with identity mapping, and global average pooling followed by a fully connected classifier for diabetes prediction

Table 1: Impact of data augmentation on classification accuracy, precision, recall, and F1-score for ResNet50, ConvNeXtBase, and the ensemble model, showing significant performance enhancement after augmentation

Model	Accuracy (%)		Precision (%)		Recall (%)		F1-score (%)	
	Without augmentation	With augmentation	Without augmentation	With augmentation	Without augmentation	With augmentation	Without augmentation	With augmentation
ResNet50	77.55	96.28	76.77	95.00	75.00	95.96	84.51	95.48
ConvNeXtBase	73.47	97.93	83.33	100.00	75.7	95.41	79.37	97.65
ResNet50 + ConvNeXtBase	69.39	99.12	82.14	98.78	69.70	99.39	75.41	99.08

incorporating augmentation, the models attained better generalization and classification accuracy. Among standalone architectures, ConvNeXtBase achieved the highest accuracy of 97.93%, with perfect precision (100%) and a strong F1-score of 97.65%, followed closely by ResNet50 with 96.28% accuracy. Ensemble methods further improved predictive performance by leveraging complementary feature representations. Among all combinations, the ConvNeXtBase + ResNet50 ensemble yielded the highest overall classification performance with 99.12% accuracy, 98.78% precision, 99.39% recall, and 99.08% F1-score, showing a clear advancement over individual models. The confusion matrix of the proposed model given in Figure 6a illustrates minimal false classifications. Out of 173 diabetic images, 171 images are classified correctly, whereas out of 169 images, 167 are accurately classified as nondiabetic. The receiver operating characteristic curve shown in Figure 6b exhibits an area under the curve approached 0.99, confirming excellent separability of class distributions and superior model generalization.

Model validation

The generalization performance of the proposed ensemble model was robustly assessed using 5-fold cross-validation. The dataset was partitioned into five equal folds, with the model iteratively trained on four folds and validated on the remaining fold. Final classification metrics were computed by averaging the results across all five folds. As shown in Table 2, the mean accuracy of 97.45% ± 0.86% represents the average classification accuracy, while the standard deviation reflects the variation in prediction performance between folds. The low deviation value indicates that the model maintains stable and reliable classification behavior across different training–testing splits, demonstrating strong consistency and reduced susceptibility to data partitioning bias. The model achieved a mean accuracy of 97.45% ± 0.86%, mean precision of 95.98% ± 2.27%, mean recall of 98.80% ± 1.07%, and mean F1-score of 97.35% ± 0.93%, demonstrating high robustness and consistent generalization across all folds.

Discussion

The experimental findings indicate that integrating modern transformer-inspired convolutional designs, such as ConvNeXtBase, with classical residual learning ResNet50 significantly enhances energy information discrimination from biofield images. ConvNeXtBase's hierarchical spatial representation effectively captures subtle textural and energy-based patterns, while ResNet50 ensures robust gradient propagation for deeper contextual learning, leading to a synergistic ensemble effect. The remarkable 99.12% accuracy demonstrates that combining diverse architectural philosophies minimizes model-specific bias and improves decision reliability. Comparatively lower performance from ensembles such as VGG16-based combinations suggests that older architectures may struggle with complex biofield feature variability. The high recall of the best ensemble highlights its potential utility in clinical screening scenarios, where missing diabetic cases could have critical implications. The strong cross-validation results further confirm that the proposed model is resilient to dataset variations.

Overall, these findings establish the ensemble of ConvNeXtBase and ResNet50 as a highly promising AI-driven decision support tool for biofield-based diabetes identification. While the model showed promising segmentation and classification performance, its findings serve as an initial foundation rather than a finalized diagnostic system. Further validation on larger, diverse, multicenter datasets along with collaboration with medical and biofield domain experts is essential to confirm the model's clinical relevance and ensure reliable interpretation of biofield image data.

Conclusions

This proof-of-concept study investigated whether biofield patterns captured from the pancreatic region can support noninvasive differentiation between diabetic and nondiabetic subjects. The findings demonstrate that deep learning-based analysis can successfully extract discriminative energetic

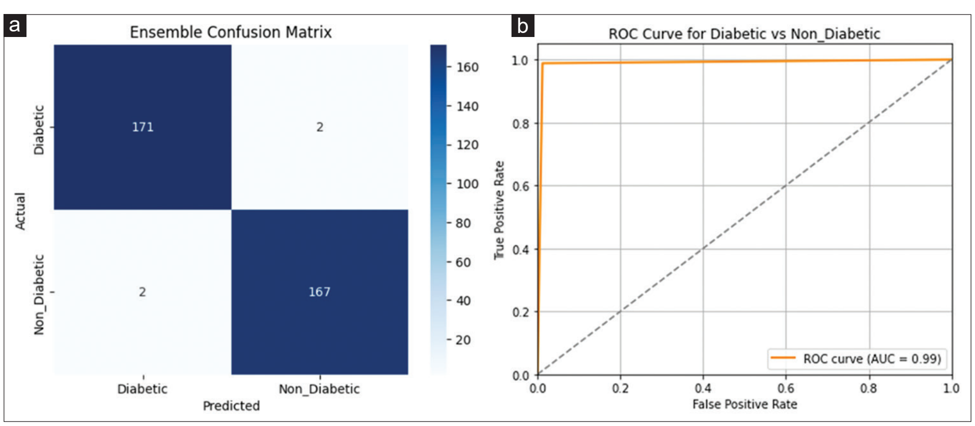

Figure 6: (a) shows the confusion matrix. (b) presents the Receiver Operating Characteristic (ROC) curve of the proposed ConvNeXtBase + ResNet50 ensemble model. The model demonstrates minimal false classifications and an area under the curve (AUC) approaching 1.0, indicating strong discriminative capability between diabetic and non-diabetic subjects

Table 2: Five-fold cross-validation performance of the proposed ConvNeXtBase + ResNet50 ensemble model for diabetic versus nondiabetic biofield image classification

Fold	Accuracy (%)	Precision (%)	Recall (%)	F1-score (%)
1	98.02	96.51	99.55	98.00
2	96.04	92.04	100.00	95.85
3	98.24	97.76	98.64	98.20
4	97.58	96.38	98.61	97.48
5	97.36	97.22	97.22	97.22
Mean	97.45	95.98	98.81	97.35

signatures from PIP images, indicating the feasibility of automated biofield interpretation as an assistive diagnostic tool.

In addition to the classification framework, clustering-based segmentation provided valuable insights into localized energy variations associated with the pancreas, highlighting the broader utility of biofield imaging in complementary and alternative medicine. Future research will focus on extending the methodology to multiple anatomical regions to detect systemic energetic imbalances across chakras and meridians. Such advancements could lead to a more holistic diagnostic ecosystem integrating physical, psychological, and emotional dimensions of health, ultimately contributing to improved early screening and well-being assessment.

Acknowledgment

We sincerely acknowledge the IBERC, Thane West, Maharashtra, India, for their valuable support in facilitating experimental validation and granting access to the dataset used in this study. Their commitment to maintaining scientific rigor greatly strengthened the research outcomes. We also extend our appreciation to the reviewers for their constructive feedback and thoughtful evaluation, which significantly improved the clarity, quality, and overall impact of this work.

Financial support and sponsorship

Nil.

Conflicts of interest

There are no conflicts of interest.

References

1. Deo A. Aabhamandal. 2nd ed. Kopari, Thane: Biofield Evaluation; 2017.
2. Chhabra G, Prasad A, Marriboyina V. Implementation of aura colourspace visualizer to detect human biofield using image processing technique. J Eng Sci Technol 2019;14:892-908.
3. Chhabra G, Prasad A, Marriboyina V. Future trends of artificial intelligence in human biofield. Int J Innov Technol Explor Eng 2019;8:3809-14.
4. Chhabra G, Onyema EM, Kumar S, Goutham M, Mandapati S, Iwendi C. Human emotions recognition, analysis and transformation by the bioenergy field in smart grid using image processing. Electronics 2022;11:4059.
5. Gornale SS, Patil SS, Deo A, Kumar S. Quantitative Analysis of Biofield Energy Imbalance through Color Segmentation and Classification Using Machine Learning Techniques. In: 2024 IEEE 9th International Conference for Convergence in Technology (I2CT). Pune, India; 2024. p. 1-5.
6. Rubik B, Muehsam D, Hammerschlag R, Jain S. Biofield science and healing: History, terminology, and concepts. Glob Adv Health Med 2015;4:8-14.
7. Bryndin E, Bryndina I. Technological diagnostics of human condition according to spectral analysis of biofield. Adv Biosci Bioeng 2019;7:50-4.
8. Joy JA, Rudrahithlu SK, Joy, M. A Literature Review on Energy Healing Techniques and Biofield – Detection and Scientific Analysis. Int J Eng Appl Comput Sci 2022;04(03). doi: 10.24032/ijeacs/0403/002.
9. Shanmugapriya B, Rajesh R. Understanding Abnormal Energy Levels in Aura Images. In: Proc ICGST AIML-11 Conf. Dubai, UAE; 2011.
10. Chiang Lee H, Wah Khong P, Ghista D. Bioenergy based medical diagnostic application based on gas discharge visualization. Conf Proc IEEE Eng Med Biol Soc 2005;2005:1533-6.
11. Srivastava S, Bhargava S, Kumari N. Effectiveness of chakra balancing on physical well-being: A multiple case study research. Cah Magellanes NS 2024;6:6402-410
12. Huang WL. The importance of treating energy imbalances and chakras replenishment for prevention and treatment of cancer. Arch Cancer Res Clin Imaging 2020;3(1). doi: 10.33552/ACRCI.2020.02.000551.
13. Yakovleva EG, Korotkov KG, Fedorov ED, Ivanova EV, Plahov RV, Belonosov SS. Engineering approach to identifying patients with colon tumors on the basis of electrophotonic imaging technique data. Open Biomed Eng J 2016;10:72-80.
14. Narayanan CR, Korotkov K, Srinivasan TM. Bioenergy and its implication for yoga therapy. Int J Yoga 2018;11:157-65.
15. Sharma N, Aggarwal LM. Automated medical image segmentation techniques. J Med Phys 2010;35:3-14.
16. Balafar MA. Gaussian mixture model based segmentation methods for brain MRI images. Artif Intell Rev 2014;41:429-439. doi: 10.1007/s10462-012-9317-3.
17. Achanta R, Shaji A, Smith K, Lucchi A, Fua P, Süsstrunk S. SLIC superpixels compared to state-of-the-art superpixel methods. IEEE Trans Pattern Anal Mach Intell 2012;34:2274-82.
18. Ester M, Kriegel HP, Sander J, Xu X. A density-based algorithm for discovering clusters in large spatial databases with noise. In: Proc 2nd Int Conf Knowl Discov Data Min 1996. p. 226-31.
19. Ding K, Huo C, Xu Y, Zhong Z, Pan C. Sparse Hierarchical Clustering for VHR Image Change Detection. IEEE Geosci and Remote Sensing Lettrs 2015;12:577-581. doi: 10.1109/LGRS.2014.2351807.
20. Rousseeuw PJ. Silhouettes: A graphical aid to the interpretation and validation of cluster analysis. J Comput Appl Math 1987;20:53-65.
21. Myagmarsuren S. Exploring the use of silhouette score in K-means clustering for image segmentation. Int J Eng Res Technol 2024;13.
22. Calinski T, Harabasz J. A dendrite method for cluster analysis. Commun Stat 1974;3:1-27.
23. Davies DL, Bouldin DW. A cluster separation measure. IEEE Trans Pattern Anal Mach Intell 1979;1:224-7.
24. Shorten C, Khosgoftaar TM. A survey on image data augmentation for deep learning. J Big Data 2019;6:60.
25. Perez L, Wang J. The effectiveness of data augmentation in image classification using deep learning. arXiv Preprint 2017;1:1-8.
26. Pan SJ, Yang Q. A survey on transfer learning. IEEE Trans Knowl Data Eng 2010;22:1345-59.
27. Tajbakhsh N, Shin JY, Gurudu SR, Hurst RT, Kendall CB, Gotway MB, *et al*. Convolutional neural networks for medical image analysis: Full training or fine tuning? IEEE Trans Med Imaging 2016;35:1299-312.
28. Litjens G, Kooi T, Bejnordi BE, Setio AA, Ciompi F, Ghafoorian M, *et al*. A survey on deep learning in medical image analysis. Med Image Anal 2017;42:60-88.
29. Liu Z, Mao H, Wu C-Y, Feichtenhofer C, Darrell T, Xie S. A ConvNet for the 2020s. In: Proc IEEE/CVF Conf Comput Vis Pattern Recognit. 2022. p. 11976-86. doi: 10.48550/arXiv.2201.03545.
30. He K, Zhang X, Ren S, Sun J. Deep residual learning for image recognition. In: Proc IEEE Conf Comput Vis Pattern Recognit. 2016. p. 770-778. doi: 10.1109/CVPR.2016.90.
31. Gomes H, Barddal J, Enembreck F, Bifet A. A Survey on Ensemble Learning for Data Stream Classification. ACM Comput. Surv 2018;50:1-36. doi: 10.1145/3054925.

32. Rajpurkar P, Irvin J, Zhu K, Yang B, Mehta H, Duan T, *et al*. CheXNet: Radiologist-level pneumonia detection on chest X-rays with deep learning. arXiv Preprint, 2017. p. 1-7. doi: 10.48550/arXiv.1711.05225.
33. Zhou ZH. Ensemble methods: Foundations and algorithms. Chapman and Hall/CRC; New York; 2012.
34. Opitz D, Maclin R. Popular ensemble methods: An empirical study. J Artif Intell Res 1999;11:169-98.
35. Bergstra J, Bengio Y. Random search for hyper-parameter optimization. J Mach Learn Res 2012;13:281-305.
36. Snoek J, Larochelle H, Adams RP. Practical Bayesian optimization of machine learning algorithms. Adv Neural Inf Process Syst 2012;2:2951-959.
37. Xu Y, Mo T, Feng Q, Zhong P, Lai M, Chang EI. Deep learning of feature representation with multiple instance learning for medical image analysis. In: Proc Med Image Comput Comput Assist Interv (MICCAI) 2014. p. 1626-630